Nansen Environmental and Remote Sensing Center

A non-profit environmental research center affiliated with the University of Bergen

Edv. Griegsvei 3a
N-5059 Bergen, Norway
Tel: 47 55297288
Fax: 47 55200050
http://www.nrsc.no

NERSC TECHNICAL REPORT NO. 194

WEMSAR

WIND ENERGY MAPPING USING SYNTHETIC APERTURE RADAR

EUROPEAN COMMISSION FIFTH FRAMEWORK PROGRAMME

ENERGY, ENVIRONMENT AND SUSTAINABLE DEVELOPMENT

KEY ACTION 5: CLEANER ENERGY SYSTEMS, INCLUDING RENEWABLE ENERGIES

REVIEW OF WIND RETRIEVAL ALGORITHMS

DELIVERABLE D2

WEMSAR REPORT NO. 1

Investigators:

Ola M. Johannessen (coordinator), Stein Sandven, Birgitte Furevik, Kjell Kloster and Heidi Espedal

December 2000

Project partners

NANSEN ENVIRONMENTAL AND REMOTE SENSING CENTER (NERSC) Edv. Griegsvei 3a N-5059 Bergen, Norway Phone: +47 55 29 72 88 Fax: +47 55 20 00 50 e-mail: stein.sandven@nrsc.no http://www.nrsc.no	**NEG Micon** **Wind & Site Department** Alsvej 21, DK8900 Randers DENMARK Phone: +45 8710 5235 (direct). Fax: +45 8710 5004 email: lcc@neg-micon.dk	**Risoe National Laboratory** **Wind Energy and Atmospheric Physics Dept.** P.O.Box 49 DK-4000 Roskilde phone +45 4677 4677 (general) fax +45 4677 5970 Email: charlotte.hasager@risoe.dk http://www.risoe.dk/vea

Terra Orbit AS Edv. Griegsvei 3A, 5059 Bergen, Norway Tlf: +47 55 203435 Fax: +47 55 200050 Email: gfjevne@online.no	**ENEA** **Divisione Fonti de Energia Rinnovabili,** C.P.2400-00100 Roma A.D. 00060 Roma, Italy Tel.: +39-06-30483994 Fax : +39-06-30486315 http://www.enea.it/com/enea/ Email: gaetano.gaudiosi@casaccia.enea.it

TITLE **WEMSAR** - Wind Energy mapping using Synthetic Aperture Radar **Review of Wind Retrieval Algorithms**	**REPORT IDENTIFICATION** NERSC Technical report no. 194 WEMSAR report no. 1
CLIENT CEC - Research Directorate-General Energy, Environment and Sustainable Development	**CONTRACT** ERK6-CT1999-00017
CLIENT REFERENCE Jurgen Greif	**AVAILABILITY** Open
INVESTIGATORS Ola M. Johannesen (coordinator), Stein Sandven, Birgitte Furevik, Kjell Kloster and Heidi Espedal	**AUTHORISATION** Bergen: December 2000 DIRECTOR Ola M. Johannessen

Contents

Executive Summary

This report gives a brief overview of the most common wind retrieval algorithms for satellite data. Wind speed over ocean can be retrieved from several satellite instruments such as Passive Microwave radiometer, Radar Altimeter and Scatterometer. The latter instrument, which has been operational in space since the launch of ERS-1 in 1991, has been designed for ocean wind measurements. Scatterometer data provides both wind speed and direction and is currently used in operational weather forecasts. These data have all coarse resolution, tentatively 50 km, and cannot be used for wind measurements in near coastal regions.

With high resolution SAR images, which have also been available from satellites since 1991, it is possible to estimate ocean wind fields in coastal regions with resolution of a few km. For wind energy estimation in these regions, SAR provide the most appropriate satellite data. However, the possibility to retrieve wind speed depends on the performance of the algorithm. Therefore several SAR algorithms for determination of wind speed and direction have been reviewed in this report. These include the SWA algorithm proposed by Chapron *et al.* (1995), the CMOD-4 wind retrieval algorithm (Stoffelen and Anderson, 1997), the CMOD-IFR2 (Quilfen et al., 1998), the VIERS algorithm of University of Hamburg and the NORUT algorithm (Engen and Johnsen, 1995) . The SAR wind algorithm review in this chapter is to a large extent based on a recent report by Jenkins et al., (1998) where state-of-the-art SAR ocean imaging and interaction models were studied. Also results of the COASTWATCH experiment, where SAR wind retrieval was investigated and evaluated against in situ ship observations (Korsbakken et al., 1998) have been important in this review.

The CMOD-4 algorithm is chosen for the use in this project. It is relatively easy to use, based on PRI images as input. It is very important, however, that correct calibration information is used so that absolute backscatter coefficients can be derived. The CMOD-4 algorithm will be used to analyse more than 50 ERS SAR images from the three test sites in Norway, Denmark and Italy. SAR derived wind speeds will then be compared with in situ wind measurements and the overall capability of SAR to estimate wind speeds in coastal regions will be assessed.

Project summary

Objectives

The overall objective is to investigate, validate and demonstrate the potential of satellite-based synthetic aperture radar (SAR) to map wind energy in offshore and near-coastal regions for potential wind turbine siting. The value of the SAR observations can be enhanced in combination with scatterometer, altimeter, model information and in situ data.
The WEMSAR tool will introduce satellite radar data into a system for selecting optimum locations for wind turbine parks. The method involves starting with mesoscale models, going via micro-siting models, and to satellite scatterometer (50 km resolution), altimeter (7 km resolution) and SAR (400 m resolution). This will provide high spatial resolution wind information for wind turbine siting, and thus improve cost-effectiveness when developing the renewable wind energy source. WEMSAR will also improve the exploitation of Earth Observation data.

Description of the work

The project consists of the following work packages;

- Implementation of existing algorithms for wind data retrieval from satellite radars, based on a literature search.
- Satellite data from SAR, altimeter and scatterometer will be obtained, processed and analysed, and wind information obtained. Validation of SAR wind energy retrieval capabilities will be performed.
- The micro-siting model will be tuned for optimal integration in the WEMSAR tool.
- Development of an integrated WEMSAR tool for optimum data synergy for maximum site selection efficiency. The tool will include information from mesoscale and micro-siting models, and satellite data. Integration with computer models covering land and topography, and integration in a Geographic Information System (GIS) will be tested. The tool will be streamlined according to user requirements.
- WEMSAR validation. For three test sites a WEMSAR wind atlas will be produced and compared against in situ data.
- Production of a marketing plan including a cost/benefit assessment for identifying potential customers, where the customers operate and the time frame of their projects. This task includes planning and initiation of product exploitation.

Expected Results and Exploitation Plans

The development of the WEMSAR tool and testing in three test sites. Results should demonstrate the usefulness of the proposed tool and provide valuable information for cost-effective use of wind energy.
The project web site is: http://www.nrsc.no/WEMSAR.

1. Introduction

Satellite microwave instruments are well suited to measure global sea-surface winds over the ocean. Both active and passive microwave techniques are used. Passive microwave radiometers measure the effect of wind on the emissivity of the sea-surface while active microwave systems measure the return signal from pulses which are emitted from the satellites and scattered 180° at the sea surface . There are three types of active microwave

instruments: scatterometer, SAR and altimeter, which all measure the backscattered signal from the sea-surface. The strength of this signal is mainly determined by the presence of wind-generated capillary waves (of size near the wavelength of the microwaves, which is typically a few cm). Capillary waves are generated by the near-surface wind, and their amplitude generally increase with increasing wind speed. Depending on instrument type, one or both wind parameters (speed and direction) can be derived, using selected algorithms on the raw data.

In general, the satellite platforms for the instruments described above use near sun-synchronous polar orbits. The satellite altitude is normally near 800 km and inclination is near 99°. Topex/Poseidon with radar altimeter deviates somewhat from this orbit constellation with 1300 km altitude and 66° inclination.

2. Wind speed from Passive Microwave Radiometer

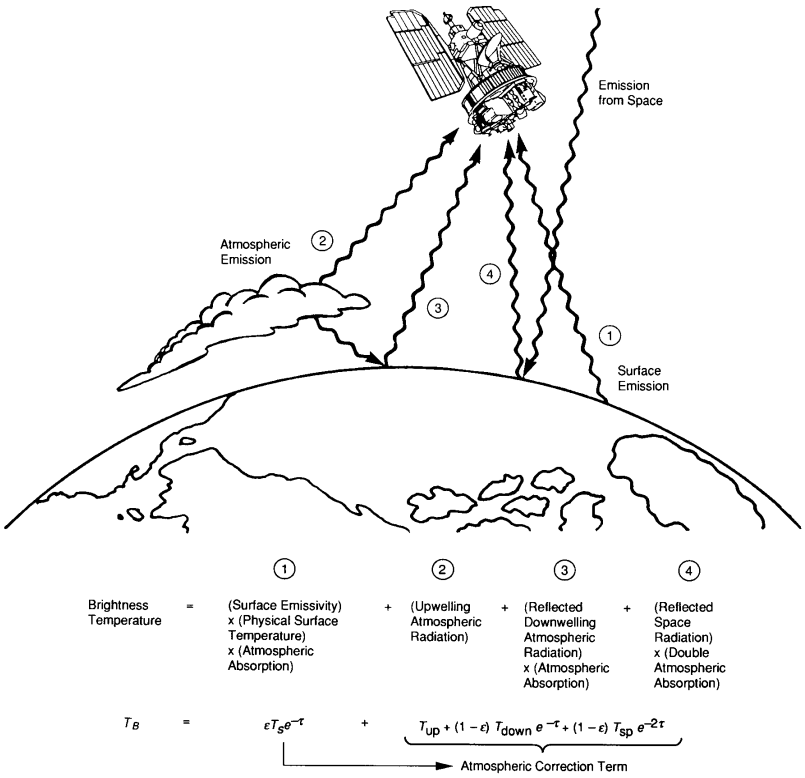

Figure 1. The main components of the brightness temperatures observed by Passive Microwave radiometer in satellites, expressed by the radiative transfer equation (Steffen et al., 1992.)

Passive microwave radiometers, which have been operational in satellites since 1978, measure the emission from the earth surface as illustrated in Fig. 1. The currently operating instrument, the Special Sensor Microwave Imager (SSM/I), is a 7-channel microwave radiometer with 4 frequencies (19 - 85 GHz) and 2 polarizations (V and H). Several geophysical parameters can be derived, over the oceans such as sea-ice concentration and ice age (FY and MY), oceanic wind speed, atmospheric integrated water vapour, and cloud liquid water. Emission will generally increase with the wind speed and depends also on surface temperature. By combining several channels, the effect of temperature is eliminated. Channel

resolution is frequency dependent, from 15km at 85GHz to 60km at 19GHz in a 1400km swath. The 85 GHz channel is noisy due to atmospheric effects.
The wind speed algorithm in use was named "Global D-Matrix Algorithm" (Hollinger 1989), it gives the speed in the range 3 -25 ms^{-1} with an accuracy of ±2 ms^{-1} and a resolution of 25 km. Daily browse gif-files of windspeed (from Feb.98) on global maps, for ascending and descending orbits separately, are found at: ftp//ghrc.msfc.nasa.gov/pub/browse/ssmi-f13/current-products (f13 can also be f14). HDF-files for global gridded data (last 36 days at ftp-site) and for swath data (last 10 days at ftp-site) are also available.

3. Scatterometer wind fields

The scatterometer on the ERS satellites, which have been in operation since 1991, measures the backscatter coefficient (σ^0) in several look-directions in order to obtain both wind speed and direction, as shown in Fig. 2. Frequency is C-band and polarisation is VV. Backscatter increases with wind speed and it is variable with wind direction (measured relative to the instrument look-direction). Three antennas with different look-directions are used (called the fore, mid and aft beams). Resolution is 50km in a 500km swath.
Another scatterometer is SeaWinds which was launched on NASA's QuikSCAT satellite in June 1999. Sea Winds uses a one meter rotating dish antenna making circular scans with two spot beams of 46° and 52° incidence angles. One beam is V-polarised and the other is H-polarised. The frequency is 13.4 GHz. The outer swath is 1800 km and basic resolution is 25 km. By special processing using both beams, a resolution of 12.5 km can be achieved (Yueh 2000).

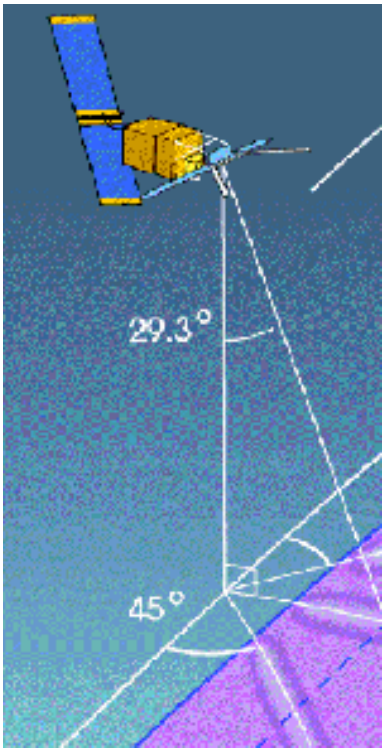

Figure 2. Geometry of the ERS scatterometer showing the three look directions

The backscatter coefficient is computed using on of several available so-called "models" between wind and backscatter, e.g. CMOD4 (Stoffelen and Anderson, 1997), IFREMER-model (Quilfen et al., 1998). The model gives σ^0 as function of wind speed, wind direction, and incidence angle. Algorithms are used to invert this model to give the wind speed and direction, with input of σ^0 from the 3 beams. These data are used in weather forecasts from the European Center for Medium-range Weather Forecasts (ECMWF). An example of a wind field over the Greenland Sea on September 1, 1995 as measured by the ERS-1 Wind Scatterometer is shown in Fig 3., together with the SAR coverage of the ERS-2 which was flying about 30 minutes after ERS-1 in the Tandem phase.

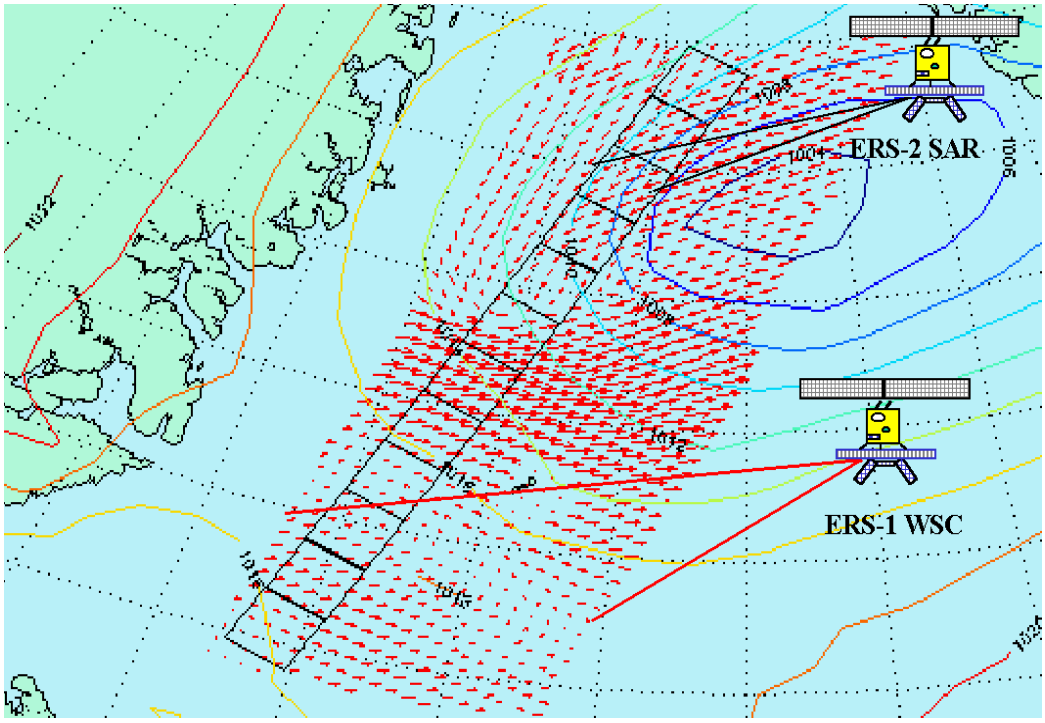

Figure 3. ERS-1 Scatterometer and ERS-2 SAR coverage in the Greenland Sea during the ERS Tandem Phase. Red arrows indicate the wind field as measured by the scatterometer, isobars are from the DNMI hindcast database (Furevik and Korsbakken, 2000).

.

From Quickscat the basic products made are: 1) σ^0 over all surfaces, 2) wind vectors over open ocean (merged Level 2A/2B product). Wind direction ambiguity removal is done using NCEP (National Center of Environmental Prediction) global forecast wind fields. An example of a global wind field is shown in Fig. 4. Mean accuracy is approximately $2ms^{-1}$ in speed (range 3 -20 m/s), and 20° in direction. Reliable wind retrievals are made over the dual-beam inner swath. In the outer swath, rapid degradation takes place as the azimuth difference diminishes. Wind products should be used with caution in the outer swath. Measurements are accurate within approx. 25 km of the coastline. A land mask of 30 km margin was found to be appropriate for all products.

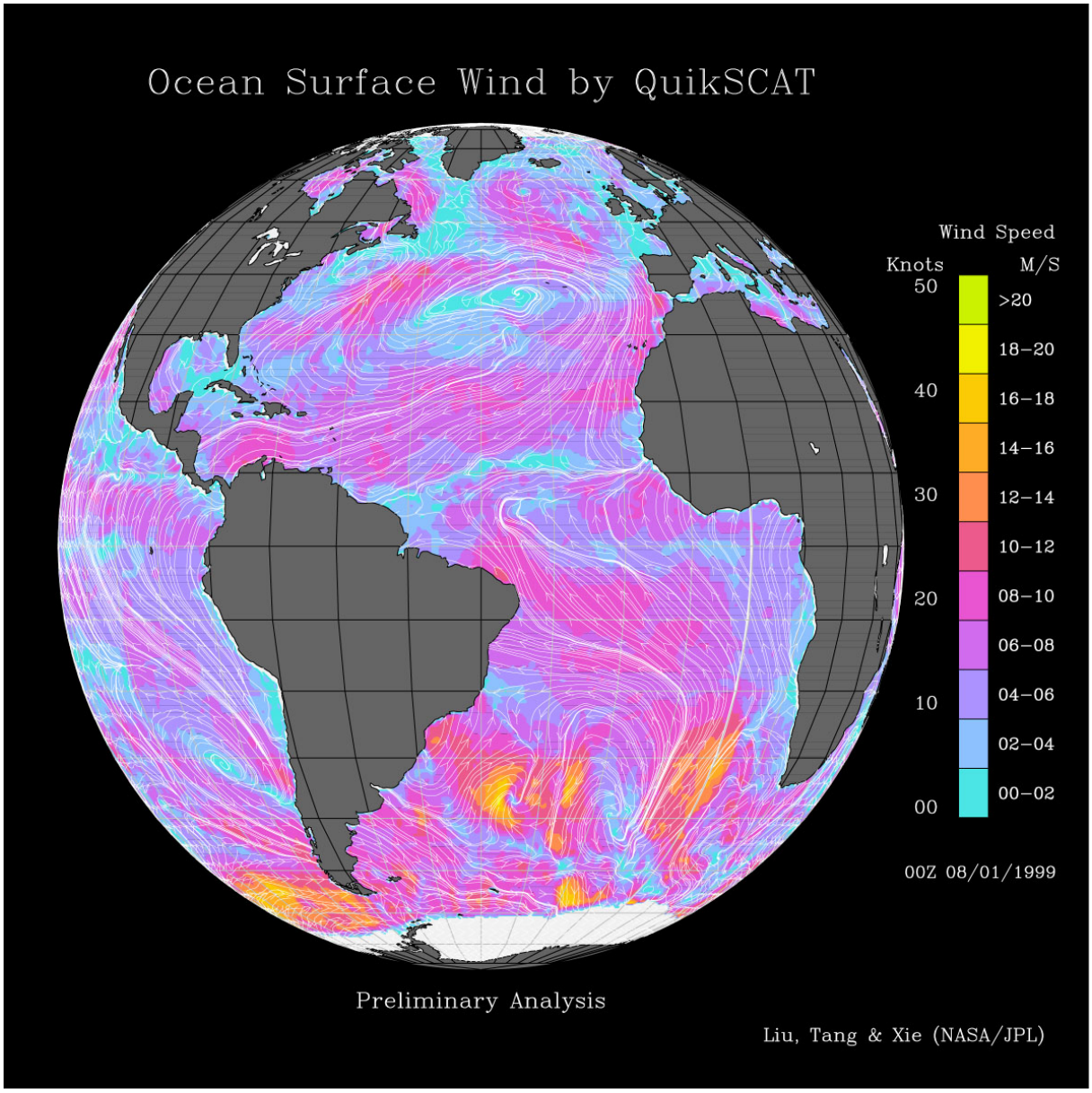

Figure 4. Example of global wind speed (colour) and direction (vectors) from Quikscat.

Research products are produced by JPL and distributed to the science community within 2 weeks. Scatterometer Science products are distributed through JPL PO.DAAC (Physical Oceanography Distributed Active Archive Center) at : http://podaac.jpl.nasa.gov.

Operational NRT (near real time) products are produced at NOAA within 3 hours for the international met. community. NRT wind is processed from fore- and aft-sigma0 from both beams (standard science level 2B algorithm). Beam balance is tuned to NCEP one-degree analysis, bias relative NCEP is thus near zero.

The NRT products for operational weather forecasting and modelling organizations contain both wind and σ^0. It is distributed by NOAA/NESDIS in the BUFR format for operational users. Ocean surface wind vector data on a regular 0.5° x 0.5° global grid between 75 S to 75 N latitude (a subset of the NRT data) is available from:

ftp://ftp-airsea.jpl.nasa.gov/pub/www/DATA/QUICKSCAT

Files are available daily at 00z and 12z from 03.Sep.99 (w/ some omissions). New files are available within approx. one day of real-time.

4. Wind speed from radar altimeters

The radar altimeters on ERS and Topex/Poseidon, operating since 1991 - 1992, measure the shape and strength of a pulse that is reflected from the ocean in the nadir direction and use these data primarily to estimate sea surface heights. The data, which are only obtained along the nadir line, can also be used to derive wind speed and wave height. Wind speed can be estimated because the pulse strength is wind speed dependent. The pulse is strongest from a smooth surface (low wind) with near-specular reflection. Increasing wind will cause the signal to be more diffusely reflected and the proportion returned to the satellite will be reduced. The radar altimeters are pulse-limited, providing data with resolution of about 6km along the flight direction, increasing somewhat with increasing wave-height.
A widely used operational wind speed algorithm is the empirical "Chelton-Wentz algorithm" (Witter and Chelton 1991).The performance of this and other algorithms (Fig. 5) is described by i.e. Dobson (1995) and Gourrion (2000). Improved algorithms have been developed by Anderson (2000).

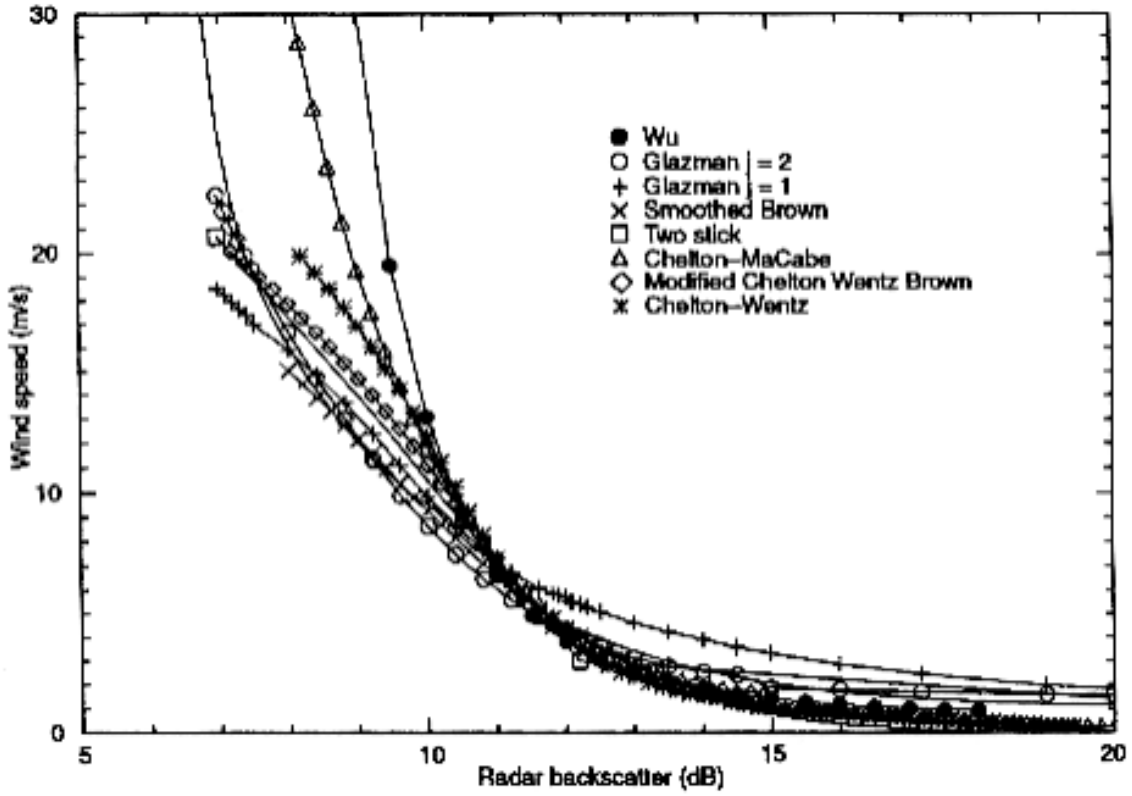

Figure 5. Comparison of various algorithms for wind speed retrieval from radar cross section of altimeter data (Dobson, 1995).

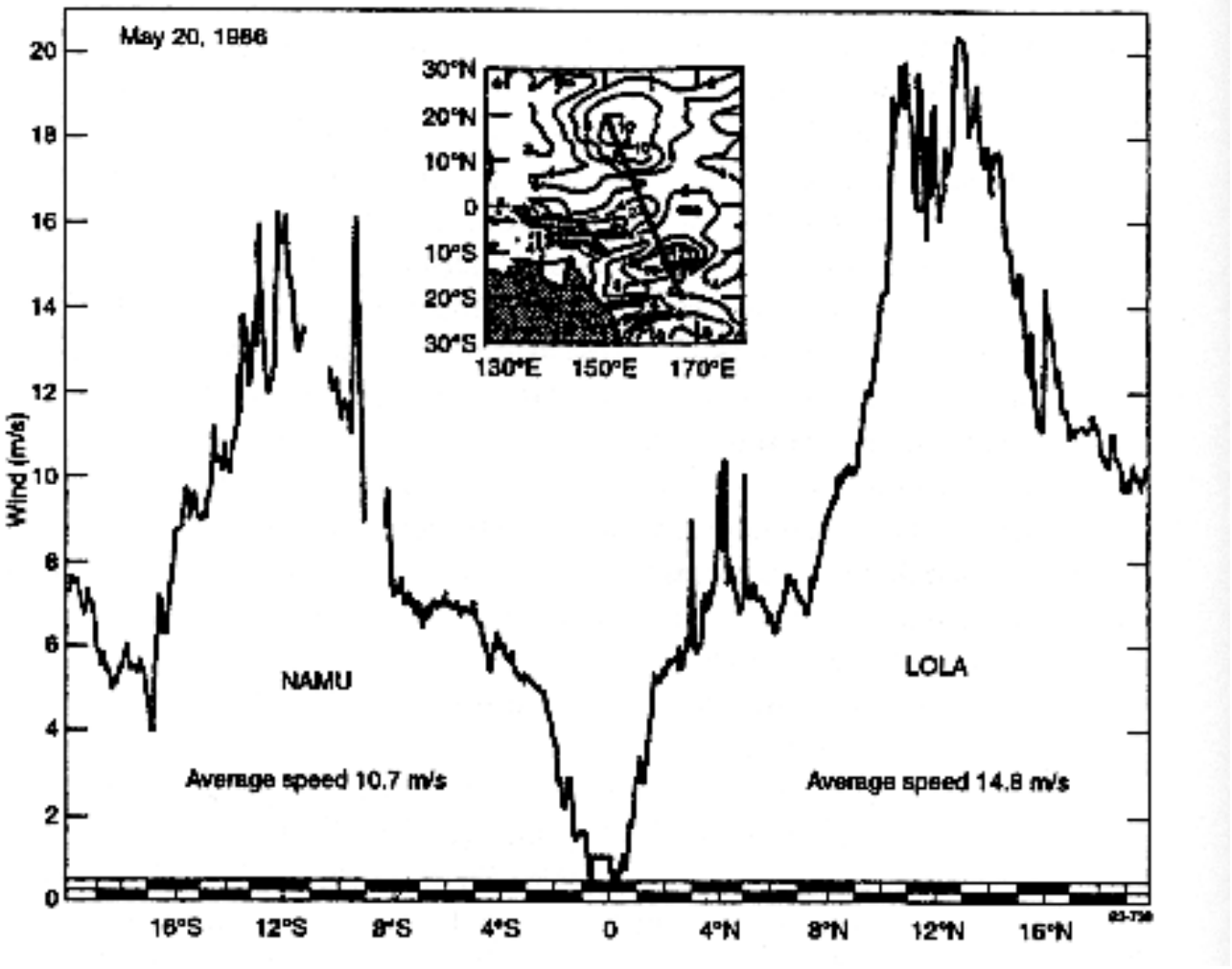

Figure 6. Example of average wind speed taken along a Geosat altimeter track across the equator in the western Pacific where two cyclones occurred in May 1986. (Courtesy D. L. Porter, 1990).

5. Wind from Synthetic Aperture Radar (SAR)

The ERS SAR system provides images of backscatter coefficients σ^0, (normalised radar cross section, NRCS), which can be used to calculate wind speed and direction in a 100 km wide swath as shown in Fig. 7. The coherent noise, called speckle, is as large as ± 3dB for highest resolution (one-look). The resolution is 30 m with 3-looks (with ± 2 dB noise in sigma0) in a swath of 100 km. Wind vector accuracy will increase but the resolution will be poorer with more looks (more averaging). 30 m resolution PRI images with values that can be transformed to σ^0 using given calibration equations (Laur 1997) are available from ESA. RADARSAT ScanSAR images have also been introduced in estimating wind speed in US coastal areas (Thompson and Beal, 2000; Monaldo, 2000).

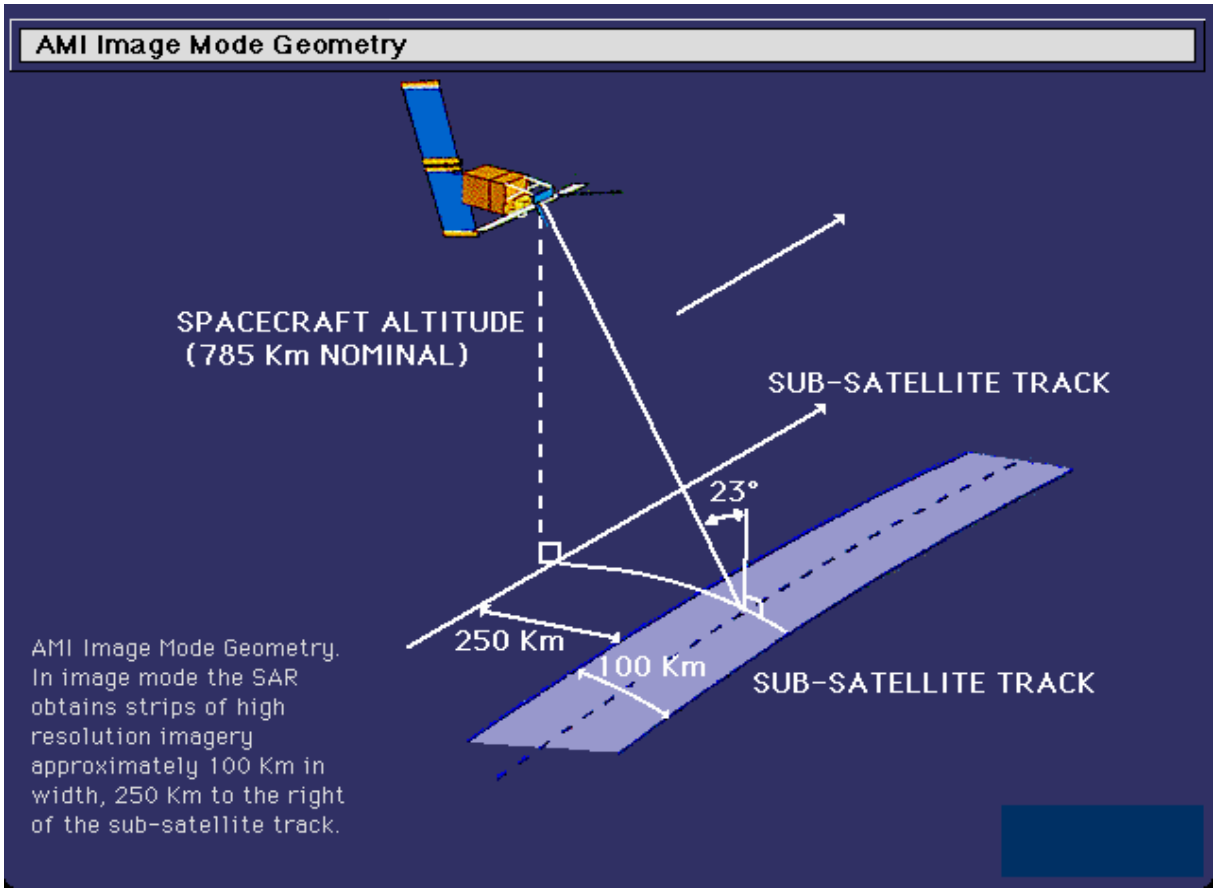

Figure 7. ERS SAR imaging geometry

This section gives a brief description of the wind speed retrieval algorithm proposed by Chapron *et al.* (1995), the CMOD4 wind retrieval algorithm (Stoffelen and Anderson, 1993), the CMOD-IFR2 (Quilfen et al., 1998), VIERS of University of Hamburg and the NORUT algorithm (Engen and Johnsen, 1995) . The SAR wind algorithm review in this chapter is to a large extent based on a recent report by Jenkins et al., (1998) where state-of-the-art SAR ocean imaging and interaction models were studied. Also results of the COASTWATCH experiment, where SAR wind retrieval was investigated and evaluated against in situ ship observations (Korsbakken et al., 1998) have been important in this review.

- ***SAR Wind Algorithm***

The SAR Wind Algorithm (SWA) proposed by Chapron *et al.* (1995) is empirically derived. The relation is between the smearing effects in the SAR image (Hasselmann and Shemdin, 1982), image statistics and the wind field. Smearing effects tend to increase the coherence (correlation length) of the radar returns in the spatial image domain and influence on the spectral properties of the SAR image. The latter can be used only to estimate the wind speed. In case of a fully developed sea the empirical relation, based on evaluation of 1200 SAR wave-mode imagettes with a central incidence angle of 20.2° is given by Chapron *et al.* (1995) as

$$U_{10} = 4.75 \left| \frac{\lambda_c - 30m}{110} \right| ms^{-1},$$

where U_{10} is the wind speed at 10 m above the surface and λ_c is the wave-induced azimuth cut-off wave length. Assuming a Gaussian shaped low pass filter for the azimutal cut-off, the cut-off wavelength can be estimated from the auto covariance function (ACF) derived from an inversion of the SAR image power density spectrum (the Wiener-Khinchin theorem). As proposed by Chapron *et al.* (1995) the ACF can be regarded as a sum of the narrow peak due to spatial resolution and a broadened `shoulder' corresponding to the Gaussian shaped filter (in the spectral domain) defined as $c(x) = \exp[-(\pi x/\lambda_c)^2]$, where x is the lag in the ACF. A Gaussian function $f(x) = \exp[-(ax)^2]$ is then fitted to the ACF in the azimuth direction over the broadened `shoulder' part of the function. In return, λ_c is then obtained from the relation $f(x) = c(x)$.

5.2 The NORUT algorithm

At NORUT information technology Ltd., Norway, an algorithm is developed from the SWA method. This method uses spectral information from pairs of single look SAR images to retrieve ocean wave spectrum (Engen and Johnsen, 1995). Using this method it is possible to extract both wind speed and direction from SAR without *a priori* knowledge and without ambiguity in the wind direction. The method is used at Tromsø Satellite Station in their 5 km x 5 km wind product form SAR (Engen et al., 1998).

5.3 The CMOD-4 and CMOD-IFR2 algorithm

The CMOD-4 and CMOD-IFR2 wind retrieval models are developed for the ERS-1 C-band scatterometer but it is also shown to give good estimates of wind speed when applied to ERS-1 SAR images (Johannessen et al., 1994; Vachon and Dobson, 1996; Vachon et al., 1995, Furevik and Korsbakken 2000). The model was developed for deep sea conditions, and is running operationally at several meteorological centres. CMOD-4 is empirically tuned to ECMWF wind fields, while CMOD-IFR2 is tuned to buoy data.

The C-band algorithm CMOD-4 gives a theoretical σ^0 value as a function of relative wind direction ϕ ($\phi = 0$ for a wind blowing against the radar), and local incident angle (α) of the illuminated area expressed as

$$\sigma^0 = B_0[1+B_1\cos\phi+ B_2\cos(2\phi)].$$

The coefficients B_0, B_1 and B_2 depend on the radar beam incidence angle (α) and wind speed. The accuracy in the model is given to 20° in wind direction relative to the radar look direction, and 2 m/s in wind speed. The CMOD-4 model is derived for a neutral stratification. In order to compute the wind speed (U_{10}) from the radar backscatter accounting for the stratification (ΔT) in the atmospheric boundary layer (ABL) the CMOD-4 derived wind speed must be

modified. A correction for this can be derived from expressions relating unstable and stable stratification to neutral stratification as suggested by Wu (1993) The saturation effect of the analogue to digital conversion (ADC) in the satellite is described by Laur et al. (1993), Meadows and Willis (1995) and Scoon (1995). The effect is strongest over ocean in the near range and increases with radar backscatter intensity (i.e. at high winds). It leads to an underestimation of σ^0 and has to be compensated in order to properly estimate the absolute value of the radar backscatter. The absolute calibrated σ^0 is derived in accordance with a comprehensive calibration scheme provided by ESA (Laur et al., 1996) except for correction for variance in the replica pulse power.

The effect of saturation is much less severe for the ERS-2 images due to different gain settings (Lehner et al., 1996). In the future ASAR, an advanced version of the ERS SAR to be mounted on ENVISAT, the 5 bit AD-converter is replaced by an 8 bit version to avoid saturation problems completely.

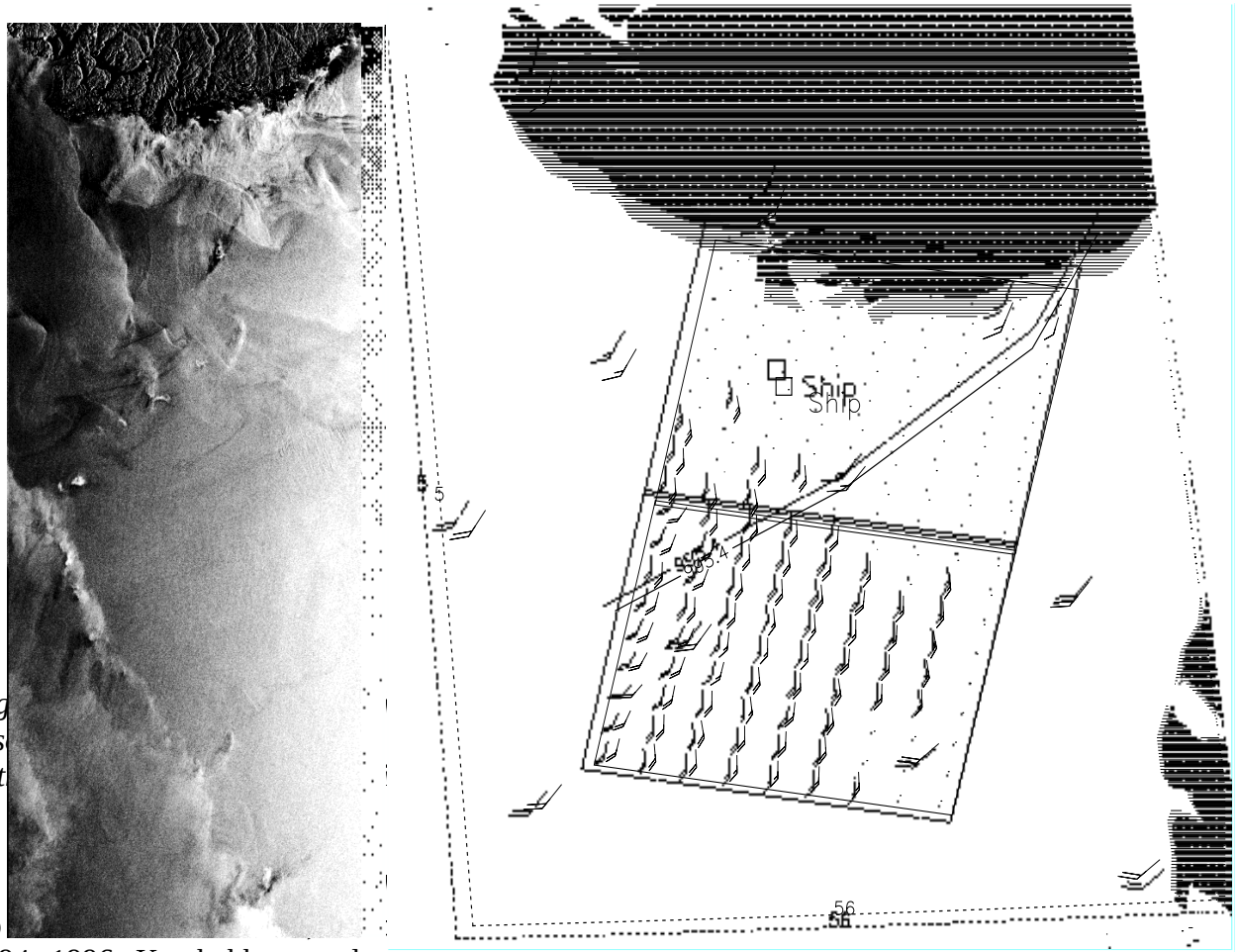

-

Fig
res
wit

-

To

1994, 1996; Korsbakken et al., 1998; Rosenthal et al., 1996). Vachon and Dobson (1996) automated this procedure by determining the wind direction from the low wave number part of the SAR spectrum ($\lambda > 2.5$ km). They found they could retrieve the wind speed and direction with an accuracy of 1.5 m/s and 24°, respectively, for winds between 3 and 12 ms^{-1} (with a 180° ambiguity).

The wind direction can also be estimated from the CMOD-4 model for different incidence angles provided the wind speed, derived from the SWA method, can be associated with the corresponding measured radar backscatter (σ^0) (Kerbaol and Chapron 1996; Korsbakken 1996). In such cases four solutions, i.e. two pairs, each with a 180° ambiguity can be found, except in the cases when the direction is close to directly upwind or downwind, for which

only one pair is found. (Note that for the three beam scatterometer on ERS-1/2 the number of solutions is reduced to a single pair with a 180° ambiguity).

The wind speed accuracy is generally of the order of ± 2 ms^{-1} for both *in situ* measured and SAR derived wind speeds. It is generally seen that the SWA, CMOD-4 and combined wind speeds are in good agreement. In particular, the SWA wind speeds in SAR images containing a fully developed wave system (no fetch limitation) are in agreement with the *in situ* observations, whereas for fetch limited seas and high wind cases the SWA method seems to underestimate the wind speed compared with the CMOD-4 and the *in situ* wind speeds. The latter suggests that the performance of the SWA method is limited to SAR images containing clear wave modulation from which the azimuth cut-off can be derived. On the other hand, the typical range of incidence angles of ERS-1/2 SAR images places no apparent constraint on the SWA method. Moreover, the estimated wind directions inverted from CMOD-4 (based on input of the SWA wind speeds and corresponding incidence angles and radar backscatter) gives relatively good results (wind direction accuracy of about $\pm 20^{\circ}$) in those cases when the performance of SWA is good. This suggests that this combination of the SWA and the CMOD-4 methods may provide a promising system for quantitative wind speed and wind direction retrievals from SAR images at high spatial resolution of 6 to 10 kilometers.

For near-coastal applications the method often fails. The short fetch and interaction of different wave fields can explain this (Korsbakken et al., 1998). Fetch limited seas can lead to underestimation of the local SWA wind retrievals since the sea state has not reached equilibrium with the local wind speed. This effect can be compensated for provided the wind direction and fetch distance can be determined. The azimuth cut off wavelength decays as a function of the wind speed at different fetch compared to a fully developed sea. The corresponding underestimation of wind speed in SWA becomes significant at 10 ms^{-1} wind speed if the seas are not fully developed. In contrast, incoming swell generated by surface winds outside the region will, of course, introduce a surface wave field that is not, again, directly in equilibrium with the local wind field. Hence, the SWA method might overestimate the local wind speed due to increased smearing.

Both the CMOD-4 and the SWA method have their strengths and weaknesses. These are qualitatively summarised in Table 1.

Table 1: Qualitative performance characteristics of the SWA and CMOD-4 methods

Characteristics	**SAR Wind retrieval algorithms**	
	SWA	**CMOD-4**
SAR image calibration	not needed	needed
ERS-1,2 SAR modes: Wave Mode Image Mode (SAR.PRI) Low resolution image (100m)	 OK OK not possible	 Limited usefulness OK OK
ENVISAT ASAR Modes: Wave mode (near range) Wave Mode (far range) Full Image Mode (near range) Full image mode (far range) Wide swath (100m) Global Mode Alternating polarisation	 OK needs to be examined OK needs to be examined not possible not possible OK	 possible (necessary calibration information is required) OK OK OK OK OK
High winds	underestimate	OK (needs to be examined)
Fetch limited seas	underestimate	OK or underestimate
Vicinity of Wind Front	underestimate for waves perpendicular to the front	OK
Boundary layer stratification	needs to be examined	can be corrected for provided ΔT is known

While image calibration is required for the CMOD-4 method it is not needed for the SWA method since the first method uses radar backscatter values while the latter uses spectral characteristics. For the different ERS-1/2 SAR modes, only the low resolution images constrain the SWA method since typical wavelengths of swell are not properly resolved in such images.

In comparison, the six different operating modes on ENVISAT ASAR (to be launched in 2001) contain no apparent limitations for the CMOD-4, except for the possibility to conduct absolute calibration of the Wave Mode products, while the SWA method undergoes the same degradation (as for the ERS-1,2 cases) when the image resolution is reduced for the wide swath and global modes. The SWA performance for the far range sector of the full image mode and the wave mode for incidence angles of about 25-40° is unclear.

The ERS wave mode data has limited analog-to-digital conversion (ADC) precision. This limits the usefulness of this mode for wind retrieval using CMOD-4 (or equivalent). In comparison it can be mentioned that this problem will not exist for ENVISAT wave mode products.

- ***The VIERS approach***

In the VIERS project a group of four research institutes in the Netherlands, the Royal Netherlands Meteorological Institute, the TNO Physics and Electronics Laboratory, Delft Hydraulics and the Laboratory for Telecommunication and Remote Sensing Technology of Delft University of Technology, attempted to develop an algorithm to retrieve wind field information from ERS scatterometer data based on physical principles. The project was financially supported by the Netherlands Remote Sensing Board (BCRS).
The VIERS algorithm (forward model) predicts the expected radar backscatter for a given wind speed and direction. To retrieve wind field information from scatterometer data this model needs to be inverted. For this purpose data assimilation inversion techniques were developed.
The Viers forward model consists of three sub-models:

- for a given wind speed at 10 m height (U_{10}) the wind stress at the water surface is computed;
- from the surface stress the full surface wave spectrum is computed;
- the wave spectrum is used to calculate the radar backscatter.

To validate the sub-models, three experiments were held in which all relevant parameters, wind speed, wind stress, wave spectra and radar backscatter, were measured in detail.
These sub-models, based on state-of-the-art knowledge of phenomena involved, are described below. For full details the reader is referred to (Janssen et al., 1995).
Wind stress module
In this sub-model a logarithmic wind profile is assumed, corrected for the stability of the air column (air-sea temperature difference):

$$U(z) = \frac{u_*}{\kappa}\left(\log\left| \frac{z}{z_0} \right| - \Psi_M\left(\frac{z}{L}\right)\right|$$

The roughness length z_0 depends on the friction velocity u_* and the period of the dominant waves P. For the stability parameter Ψ_M the Businger-Dyer expression is adopted, which gives separate parameterizations for stable ($T_{air} > T_{sea}$) and unstable ($T_{air} < T_{sea}$) conditions.
Wave module
The wave spectrum can be separated into three parts: swell, gravity waves and capillary waves. The swell part is independent of the wind and can therefore not be assessed locally from a given friction velocity. This part should be provided by an ocean wave prediction model. Fortunately, the influence of swell on scatterometer measurements is generally negligible.
The sea part for gravity waves is in this module parameterized by the JONSWAP shape

$$E_{JON}(f) = \frac{\alpha g^2}{(2\pi)^4 f^5} \exp\left| -\frac{5}{4}\left(\frac{f_p}{f}\right)^4 \right| \gamma^r$$

with the peak frequency f_p inversely proportional to the peak period P. The Phillips constant α and the peak enhancement factor γ depend only on the wave age $\xi \propto P / u_*$. The exponent r in the peak enhancement factor depends only on $f–f_p$. This gravity wave spectrum is assumed to be valid up to a frequency f_{join}, which lies between 2 and 5 Hz.
Above the frequency f_{join} the capillary regime is entered. Here the spectral form is modelled by the action balance equation:

$$\frac{dE(f)}{dt} = S(E, f, u_*).$$

It is assumed that the spectrum E is in equilibrium which means that dE/dt = 0, so that the source function S should be zero for all frequencies. In the source function the following physical phenomena are modelled separately:

- wave growth through wind input
- nonlinear 3-wave interaction
- nonlinear 4-wave interaction
- damping by wave breaking
- viscous damping
- damping by slicks

Radar backscatter module

Several backscatter models taken from the literature (Small Perturbation Method, Two-Scale model (Donelan and Pierson, 1987), `Holliday' model (Holliday, 1991, Holiday et al., 1986, 1987), Integral Equation method (Fung and Pan, 1987), Full Wave Model (Bahar, 1981a,b,c) were tested in the VIERS project using the detailed wave and radar backscatter measurements obtained in Delft wind-wave flume (first experiment). Best results were obtained with a modified two-scale model, in which the total radar backscatter σ^0 consists of a Small Perturbation Method contribution and a Physical Optics contribution.

Model inversion

To retrieve wind field information from measured ERS scatterometer data the VIERS model is inverted with the help of a cost function approach. The scatterometer provides three backscatter values σ_i, where i stands for fore-, mid- or aft-beam. For given wind speed U and wind direction ϕ the VIERS model computes three corresponding backscatter values σ_i^{model}. Furthermore, it is assumed that a first guess wind speed assessment U_{GEO} and ϕ_{GEO}, for instance computed by the ECMWF model, is available. From these data a cost function C is constructed as

$$C = \sum_i w_i\left(\sigma_i - \sigma_i^{model}\right)^2 + w_U\left(U - U_{GEO}\right)^2 + w_\phi\left(\phi - \phi_{GEO}\right)^2$$

The weights w_i are related to the expected accuracy of the measurements σ_i. The last two terms in the cost function are added to remove the upwind-downwind ambiguity and to force the retrieved wind speed to be near the initial guess model wind. The U, ϕ combination which minimizes this cost function is the retrieved wind speed.

The minimization procedure is simple but not very efficient: a table is pre-computed for wind speeds between 1 and 30 m/s with steps of 1 ms^{-1}, wind angles between 0° and 360° with steps of 15°, and radar incidence angles between 18° and 57° with steps of 1°. For this discrete set of possible wind speeds and directions all cost function values are computed and the minimum value is looked up.

5.6 Composite surface model of UHSO

An advanced composite surface model for radar backscatter calculations has been developed at the University of Hamburg. This model is based on the standard expressions of Bragg scattering theory (Valenzuela, 1879; Wright 1968; Lyzenga 1998), but it includes a number of second-order terms of the normalized radar backscattering cross section (NRCS) of the sea surface, which are obtained from a Taylor expansion with respect to the surface slopes parallel and normal to the radar look direction. This way, the composite surface model accounts for the impact of the full two-dimensional wave spectrum on the NRCS.

In addition to `tilt modulation' terms or `geometric' terms, which result directly from the Taylor expansion, the proposed model includes also `hydrodynamic' terms. These terms account for the hydrodynamic modulation of the short Bragg waves (ripple waves) along

longer waves and their resulting asymmetric distribution with respect to the surface slope, giving rise to an upwind / downwind asymmetry of the NRCS.
The proposed model was mainly developed for the simulation of radar signatures of spatially varying surface current fields over underwater bottom topography or internal waves. For this purpose, it is normally combined with a wave-current interaction model which provides hydrodynamically modulated surface wave spectra, and quantitative analyses focus on the reproduction of measured relative variations of the NRCS. However, after some dedicated (but reasonable) optimization of the parameterization of the input wave spectrum, the model is supposed to also be capable of predicting realistic absolute NRCS values for wide ranges of radar parameters and surface wind vectors. It can thus be considered as well as a more `physical' alternative to existing empirical wind scatterometer models.

5.7 Other models

In cases where the wind speed is changing rapidly in space or in time it may not be possible to assume that the wave field is in equilibrium with the wind. Although the C-band Bragg waves respond very quickly to changes in the wind, longer waves respond more gradually and may influence the backscatter through various coupling mechanisms. One attempt to incorporate these effects by modelling the energy dissipation rate for short waves as a function of the long wave spectrum is described in Lyzenga (1998).

6. Evaluation and intercomparison of the SAR models

The two SAR wind retrieval algorithms, CMOD-4 and SWA, are based on the extraction of the wind field from different parts of the ocean surface wave spectrum, in particular the medium wind wave regime and the small centimetre scale regime. Figure 9 shows a conceptual overview of the wind field estimation as further described below.
The CMOD-4 wind speed estimates appear not to be affected by fetch limited seas. Quite differently, on the other hand, this method is affected by surface boundary layer conditions such as the stratification and presence of surface films. While the former effect can be corrected for via a boundary layer model for stable or unstable stratification, the effect of the latter will always dampen the surface roughness and hence reduce the wind speed. At the same time, increased presence of surface films will attenuate σ^0 and lead to an underestimation in the CMOD4 wind speed. Quantification of the effect is difficult because the attenuation of σ^0 depends on the unknown physical parameters of the surface films. An uncertainty factor in applying the CMOD4 model to SAR data is local variations in the surface wind direction and, in turn, our assumption of a local in situ measurement to be valid in all sub-images in the imaged area. The only confidence in this assumption applies to cases where wind rows confirm the homogeneity of the wind direction.

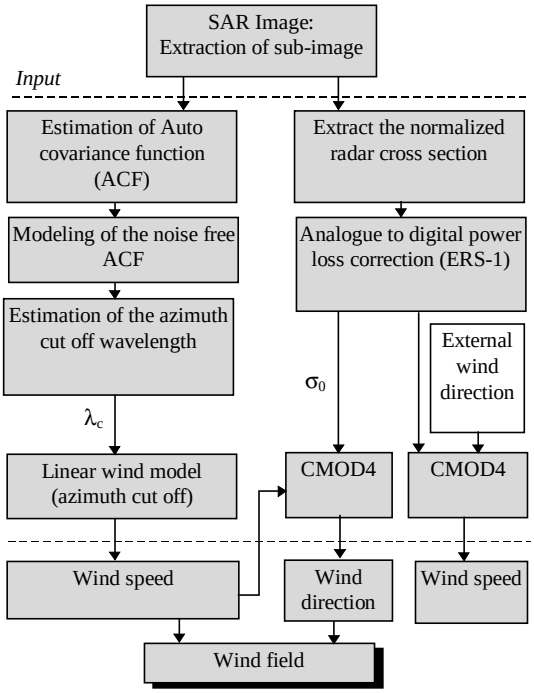

Figure 9. Conceptual overview of the SWA and CMOD-4 wind retrieval model (Korsbakken et al, 1998).

The largest errors in wind directional asymmetry in the CMOD-4 model occur if the used wind direction has positive deviations from 45°. The error estimate does not vary significantly in the range of ERS SAR incidence angles of about 19° to 26°. For the relative high wind speeds observed in most of the cases studied by Korsbakken et al., (1998) the wind direction used to derive the CMOD4 wind speed becomes a significant error source and may cause errors up to 2 ms^{-1} in the derived wind speed, if the wind direction estimate is no better than $\pm 20^{\circ}$. The CMOD-4 method may also be sensitive to rain showers affecting the radar backscatter.

A better spatial resolution than discussed before (10 x10 km) can be obtained for CMOD-4 wind speed estimates. The dependency in CMOD-4 wind speed and the σ^0 of the spatial resolution is illustrated in Figure 10 which shows the variability in σ^0 and the corresponding CMOD-4 wind speed as a function of increasing the sub-image size from 100 m to 10 km, using in situ wind data as reference.

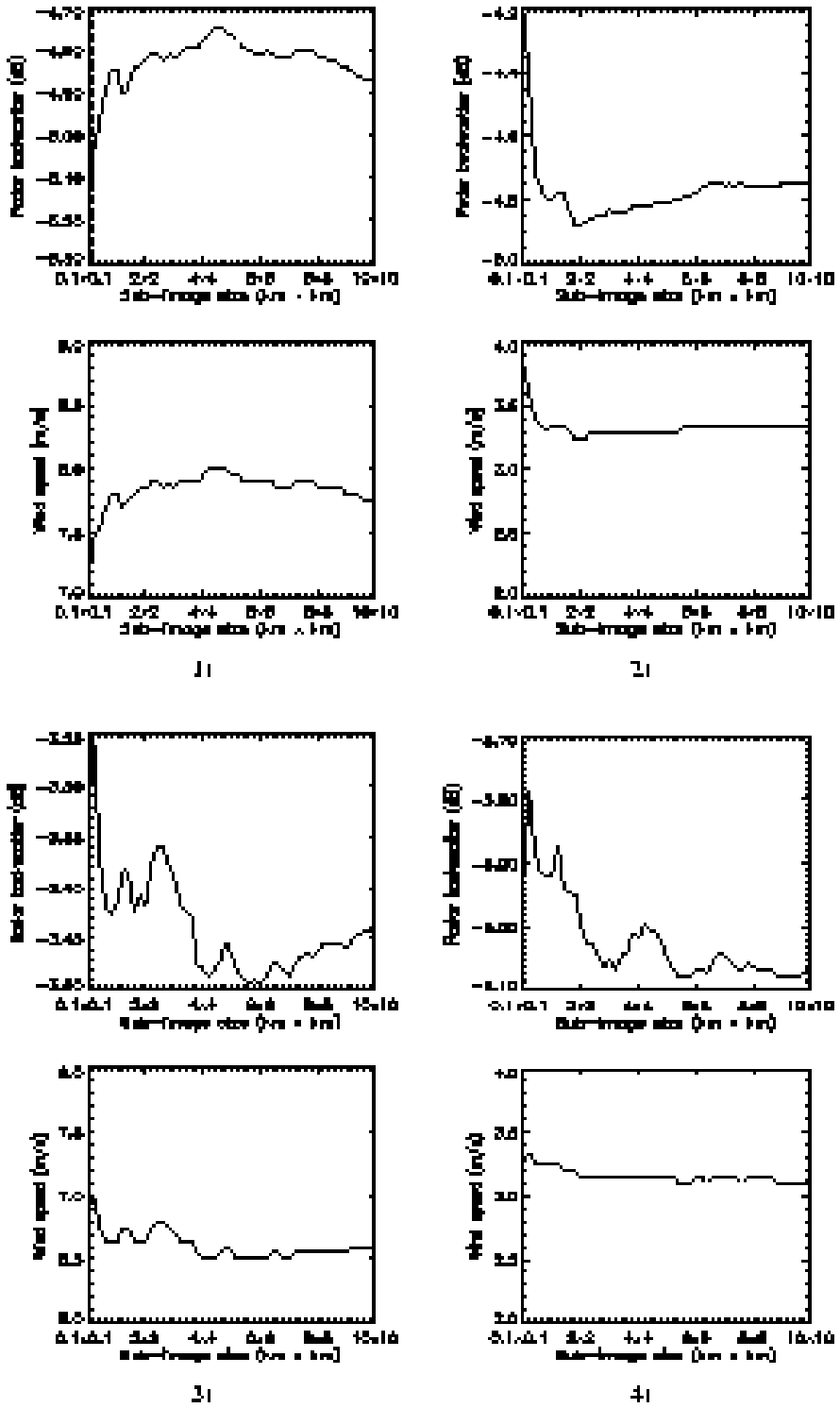

Figure 10: Plots of σ^0 and the corresponding CMOD-4 wind speed measurements as a function of sub-image size. Plots 1 (top left) and 2 (top right) are taken from the same position as the in situ measurements from R/V Håkon Mosby on 16 and 17 September 1995. Plots 3 and 4 corresponds to in-situ measurements on 23 and 27 September, respectively, in the study by Korsbakken et al., (1998)

The enlargement of the sub-images is done symmetrically around the centre pixel of 100 x 100 m located close to the in situ measurements from R/V Håkon Mosby in four of the COAST WATCH'95 data sets. Homogenous areas are chosen. The plots show a rapid convergence and small variations in σ^0 as a function of the sub-image size, and the corresponding CMOD4 winds do not change significantly with size. The latter property is important for resolving wind changes in local intense small-scale weather systems.

7 Conclusions

For more than 10 years, large-scale and global wind speed at sea surface have be estimated from Passive Microwave radiometer data as well as from Radar Altimeter, the latter only provides data along the nadir line. These instruments have been design for other purposes than wind observation and wind speed is just an additional products from these data. Scatterometer on the other hand, which has been operational since the launch of ERS-1 in 1991, has been designed for ocean wind measurements. Scatterometer data provides both wind speed and direction and is currently used in operational weather forecasts. These data have all coarse resolution, tentatively 50 km, and cannot be used for wind measurements in near coastal regions.

With high resolution SAR images, it is possible to estimate wind fields in near coastal regions with resolution of a few km. Several SAR algorithms for determination of wind speed and direction have been reviewed in this report. The NORUT algorithm is particular promising, because it gives wind speed and direction without a priori knowledge and without ambiguity in the direction. Input data are Single - Look Complex data. For the WEMSAR project we have chosen the CMOD-4 algorithm which uses PRI data as input, because all existing PRI data in the study areas could be utilized. In addition, CMOD-4 require available information on wind direction such as wind streaks, shadowing by land, etc. It is necessary, however, to pay very careful attention to the radiometric calibration of the images, including the effects of A/D converter saturation, especially for ERS-1 data. Under suitable circumstances, the directional information may be obtainable from the low-wave number part of the two-dimensional SAR spectrum. The saturation problem should be avoided in the 8-bit A/D converter to be used in ASAR on Envisat.

The effect on the backscatter coefficient of atmospheric stability, principally the air-sea temperature difference, can also be accounted for, but some more systematic study of its effects is still required as it is not yet clear whether the effect on the radar backscatter is purely due to the resulting changes in the wind stress / friction velocity.

The CMOD-4 algorithm appears to be the most practical basis for further development. It is very important that correct calibration information is always easily accessible so that absolute backscatter coefficients can be derived. Further work needs to be done to clarify the effect of short fetch and atmospheric stability: this will require detailed measurements of the surface wave field and atmospheric boundary layer properties.

8. References

Bahar, E. Full-wave solutions for the depolarization of the scattered radiation fields by rough surfaces of arbitrary slope. *IEEE Transactions on Antennas and Propagation*, 29(3):443--454, 1981a.

Bahar, E. Scattering cross sections for composite random surfaces: Full wave analysis. *Radio Science*, 16(6):1327--1335, 1981b.

Bahar, E. Scattering cross sections for random rough surfaces: Full wave analysis. *Radio Science*, 16(3):331--341, 1981c.

Chapron, B., T. E. Fouhaily, and V. Kerbaol. Calibration and validation of ERS wave mode products, Mar. 1995. IFREMER Document DRO/OS/95-02.

Dobson, E.B. "Wind speed from altimeters". Chapter 12 in Ikeda and Dobson: "Oceanographic Applications of Remote Sensing, CRC Press Inc., 492 pp, 1995.

Donelan, M. A. and W. J. Pierson. Radar scattering and equilibrium ranges in wind-generated waves with application to scatterometry. *Journal of Geophysical Research*, 92(C5):4971--5029, 1987.

Engen, G., H. Johnsen, H. E. Krogstad, and S. F. Barstow. Directional wave spectra by inversion of synthetic aperture radar ocean imagery. *IEEE Transactions on Geoscience and Remote Sensing*, 32(2):340--352, 1994.

Engen, G. and H. Johnsen, SAR-ocean wave inversion using image cross spectra, IEEE Transactions of Geoscience and Remote Sensing, 1995, 33, 4, "1047-1056",

Engen, G., K. A Høgda and H. Johnsen, A new method for wind field retrieval from SAR data, CEOS SAR workshop, WPP-138, 1998, ESA/ESTEC, 47-51

Fung, A. K. and G. W. Pan. A scattering model for perfectly conducting random surfaces. I. Model development. *International Journal of Remote Sensing*, 8(11):1579--1593, 1987.

Furevik, B. and E. Korsbakken Comparison of derived wind speed from Synthetic Aperture Radar and Scatterometer during the ERS Tandem Phase. IEEE Trans. Geosc. And Rem. Sens. Vol. 38, No. 2, pp. 1113 - 1122, 2000.

Gourrion, J. et.al.: "Satellite altimeter models for surface wind speed developed using ocean satellite crossovers". IFREMER technical report no. DROOS-2000-02, May. 2000, Plouzane, France.

Hasselmann, K. and O. H. Shemdin. Remote sensing experiment {MARSEN}. *International Journal of Remote Sensing*, 3:139--361, 1982.

Holliday. D. Backscattering of electromagnetic waves from a perfectly conducting, gently sloping surface of finite amplitude. *IEEE Transactions on Antennas and Propagation*, 39:251--252, 1991a.

D. Holliday, G. St.-Cyr, and N. E. Woods. Comparison of a new radar ocean imaging model with SARSEX internal wave image data. *International Journal of Remote Sensing*, 8:1423--1430, 1987.

Hollinger J. (ed.), 1989; "DMSP SSM/I Calibration /Validation. Final Report". July 1989, NRL, Washington DC.

Jenkins, A. D. et al. Intercomparison and Improvement of SAR Ocean Imaging Interaction Models. Final report of ESA Contract No. 11969/96/NL/CN. NERSC Technical Report no. 132, 122 pp, February 1998

Johannessen, J. A., P. W. Vachon, and O. M. Johannessen. ERS-1 SAR imaging of marine boundary layer processes. *Earth Observation Quarterly*, (46):1--5, 1994.

Johannessen, J. A., P. W. Vachon, and O. M. Johannessen. ERS-1 SAR imaging of marine boundary layer processes, Study of the Earth System from Space. *Journal of the Russian Academy of Science*, (3):79--88, 1996.

Kerbaol, V. and B. Chapron. Calibration and validation of ERS-1/2 wave mode products, 1996. IFREMER document DRO/OS/96-08.

Korsbakken, E. Quantitative wind field retrievals from ERS SAR images. Technical report, Ocean and Sea Ice Unit, Earth Sciences Division, ESTEC, ESA, Mar. 1996.

Korsbakken, E., J. A. Johannessen, and O. M. Johannessen. Coastal wind field retrievals from ERS synthetic aperture radar images. *Journal of Geophysical Research*, (C), 1998.

Laur, H., P. Meadows, J. I. Sanchez, and E. Dwyer. ERS-1 radiometric calibration.Technical report, ESA ESRIN, Frascati, Italy, 1993.

Laur H. et al.:"Derivation of sigma0 in ESA ERS SAR PRI products." ESA doc. ES-TN-RS-PM-HL09, May 1997.

Laur, H., P. Bally, P. Meadows, J. Sanchez, B. Schaettler, and E. Lopinto. Derivation of the backscattering coefficient σ^0 in ESA ERS SAR PRI products, June 1996. Document No. ES-TN-RS-PM-HL09, Issue 2, Rev. 2, ESA ESRIN.

Lecomte P.: "CMOD4 Model description". ESRIN Doc.no. ER-TN-ESA-GP-1120, Feb.1993, Frascati, Italy.

Lehner, S., J. Horstmann, W. Rosenthal, and W. Koch. Mesoscale wind measurements using recalibrated ERS-SAR images. Proceedings of the ERS workshop at IFREMER, 1996.

Lyzenga. D. R., Effects of intermediate-scale waves on radar signatures of ocean fronts and internal waves. Submitted to J. Geophys.\ Res., 1998.

Meadows, P. J. and C. J. Willis. Derivation of radar cross section coefficient in UK-PAF ERS-1.SAR.PRI products. Technical report, GEC-Marconi Research Centre, 1995.

Monaldo, F., The Alaska SAR Demonstration and Near-Real-Time Synthetic ApertureRadar Winds. John Hopkins APL Technical Digest, Coastal and Marine Applications of Wide Swath SAR, Jan - March 2000, Volume 21, No. 1, pp 58 - 67.

Porter, D. L. Geosat observations of the tropical Pacific cyclne pair of May 1986. J. Geophys. Res. 95 (D4), 3705, 1990.

Quilfen, Y., B. Chapron, T. Elfouhaily, K.Katsaros and J. Tournadre, Observation of tropical cyclones by high-resolution scatterometry, JGR, 1998, 103, "C4", "7767-7786",

Rosenthal, W., S. Lehner, J. Horstmann, and W. Koch. Wind measurements using ERS-1 SAR. In *Proc. Second Intl Workshop on ERS Applications, London, 1995 December 6--8*, pages 355--358, Noordwijk, The Netherlands, Feb. 1996. ESA Publications Division ESA SP-383.

Scoon, A. *Analysis and Interpretation of SAR Data for the English Channel*. PhD thesis, University of Southampton, May 1995.

Steffen , K., J. Key, D. J. Cavalieri, J. Comiso; P. Gloersen, K. St. Germain, I. Rubinstein. The estimation of geophysical parameters using Pasive Microwave Algorithms. In Microwave Remote Sensing of Sea Ice, ed. F. Carsey, AGU Geophysical Monograph No. 68, Chapter 10, 201 - 231, 1992.

Stoffelen, Ad and David Anderson, Scatterometer data interpretation: Estimation and validation of the transfer function CMOD4, JGR, 1997, 102, "C3","5767-5780"

Thompson, D. R. and R. C. Beal. Mapping High-Resolutin Wind Fields Using Synthetic Aperture Radar. John Hopkins APL Technical Digest, Coastal and Marine Applications of Wide Swath SAR, Jan - March 2000, Volume 21, No. 1, pp 75 - 79.

Vachon, P.W. J.A. Johannessen, and D. Browne. ERS-1 SAR images of atmospheric gravity waves. *IEEE Transactions on Geoscience and Remote Sensing*, 33(4):1014--1025, 1995.

Vachon, P. W. and F. W. Dobson. Validation of wind vector retrieval from ERS-1 SAR images over the ocean. *The Global Atmosphere and Ocean System*, 5:177--187, 1996.

Valenzuela. G. R. Theories for the interaction of electromagnetic and ocean waves---A review. *Boundary-Layer Meteorology*, 13:61--85, 1978.

Witter D.L. and Chelton D.B: "A geosat altimeter wind speed algorithm and a method for altimeter wind speed algorithm developement". J.Geophys.Res. 96, no.C5 1991 pp.8853 -8860.

Wright. J. W. , A new model for sea clutter. *IEEE Transactions on Antennas and Propagation*, 16:217--223, 1968.

Wu, J. Ripples and oceanic remote sensing. In *Proc. Environment'93*. HKUST, Hong Kong, 1993.

Yueh, Simon: "Interplay between wind ...". EOS Transactions AGU, Vol.81 No.23, 6.June 2000, pp.253.